Biomaterials 31 (2010) 4592–4599

Contents lists available at ScienceDirect

Biomaterials

journal homepage: www.elsevier.com/locate/biomaterials

Prostate cancer cell death produced by the co-delivery of Bcl-xL shRNA and doxorubicin using an aptamer-conjugated polyplex

Eunjung Kim [a], Yukyung Jung [a], Hyangtae Choi [b], Jaemoon Yang [c], Jin-Suck Suh [c], Yong-Min Huh [c], Kunhong Kim [b,**], Seungjoo Haam [a,*]

[a] Department of Chemical and Biomolecular Engineering, College of Engineering, Yonsei University, Seoul 120-749, Republic of Korea
[b] Department of Biochemistry and Molecular Biology, College of Medicine, Brain Korea 21 Project for Medical Science of Yonsei University, Center for Chronic Metabolic Disease Research, Yonsei University, Seoul 120-752, Republic of Korea
[c] Department of Radiology, College of Medicine, Yonsei University, Seoul 120-752, Republic of Korea

ARTICLE INFO

Article history:
Received 27 January 2010
Accepted 10 February 2010
Available online 4 March 2010

Keywords:
Combination cancer therapy
Co-delivery
Aptamer
Doxorubicin
Bcl-xL shRNA

ABSTRACT

We investigated the synergism between shRNAs against Bcl-xL and doxorubicin (DOX) using aptamer-conjugated polyplexes (APs) in combination cancer therapy. Synergistic and selective cancer cell death was achieved by AP-mediated co-delivery of very small amounts of DOX and Bcl-xL-specific shRNA, which simultaneously activated an intrinsic apoptotic pathway. A branched polyethyleneimine (PEI) was grafted to polyethylene glycol (PEI–PEG) to serve as a vehicle for shRNA delivery, and its surface was further conjugated with an anti-PSMA aptamer (APT) for the selective delivery of APs to prostate cancer cells that express prostate-specific membrane antigens (PSMA) on their cell surface. The APs were finally obtained after intercalation of DOX to form shRNA/PEI–PEG–APT/DOX conjugates. Cell viability assays and FACS analysis of GFP expression against PC3 (PSMA deficient) and LNCaP (PSMA overexpressed) cells demonstrated that the synthesized APs inhibited the growth of PSMA-abundant prostate cancer cells with strong cell selectivity. Consequently, IC_{50} values of APs loaded with both DOX and shRNA were approximately 17-fold less than those for the simple mixture of shRNA plus drug (shRNA/Lipofectamine + DOX). These results suggest that AP-mediated co-delivery of an anti-cancer drug and shRNA against Bcl-xL may widen the therapeutic window and allow for the selective destruction of cancer cells.

1. Introduction

Combination therapies which simultaneously administer two or more medications are common and effective ways to treat cancer [1]. A leading example is the combination of chemotherapeutic drugs that have different mechanisms of action, which have additive or synergistic effects on overcoming drug resistance, one of the major problems of current cancer treatments. A combination of drugs with different efficacies also allows the use of lower doses and can reduce intolerable side effects [2,3]. In addition, a combination of treatment modalities such as surgery, radiation therapy, photodynamic therapy, gene therapy, and/or chemotherapy is also widely considered to achieve synergistic therapeutic efficacy [4–6]. In particular, after local tumor confinement via surgery or radiation therapy, chemotherapy combined with gene therapy can kill cancer cells systemically, including cancer cells that have spread to distant sites [7–9]. Finally, combination therapy is highly useful in treating advanced cancers which are not suitable for radiation therapy or surgical treatment.

In recent decades, much effort has been applied to developing micron or sub-micron (≤hundreds of nanometers) drug carrying systems that would cause enhanced permeation and retention (EPR) to provide sustained and controlled drug release and to allow surface functionalization for targeting and increased cellular uptake. Further development of these well-tailored nanocarriers potentiates the simultaneous delivery of multiple medications, e.g., therapeutic antibodies plus chemotherapeutic drugs [10–13]. This is especially pertinent as the co-delivery of a drug plus a genetic component has superior therapeutic effects compared to the use of individual treatments alone [14–16]. For instance, the co-delivery of paclitaxel plus an interleukin-12 (IL-12)-encoding plasmid by cationic core-shell nanoparticles synergistically suppresses cancer growth [17]. Additionally, the delivery of small interfering RNAs

* Corresponding author. Tel.: +82 2 2123 2751; fax: +82 2 312 6401.
** Corresponding author. Tel.: +82 2 2228 1680; fax: +82 2 312 5041.
E-mail addresses: kimkh34@yuhs.ac (K. Kim), haam@yonsei.ac.kr (S. Haam).

0142-9612/$ – see front matter © 2010 Elsevier Ltd. All rights reserved.
doi:10.1016/j.biomaterials.2010.02.030

(siRNAs) against Bcl-2 using cationic micelle type nanoparticles sensitized cancer cells to paclitaxel, while siRNA alone had no significant cytotoxicity [18]. Of note, siRNA-mediated silencing of Bcl-2, an anti-apoptotic gene, synergized with even small amounts of doxorubicin (DOX) was successful in inducing cancer cell death [19,20]. Thus, the combination of RNAi (RNA interference)-mediated down-regulation of Bcl-xL and doxorubicin (DOX) may be a reliable therapeutic model for efficient combination cancer therapy.

In vivo gene delivery based on polycationic polyethyleneimine (PEI) has been extensively studied and huge effort has been dedicated to apply PEI/DNA complexes *in vivo*. For instance, Aigner et al. reported HER-2-specific siRNA treatment using a simple system through PEI complexation in a subcutaneous mouse tumor model and showed that PEI significantly improves the *in vivo* efficiency of siRNA [21]. Other *in vivo* approaches for siRNA based on PEI are mainly focused on intratumoral delivery of plasmid-encoded focal adhesion kinase (FAK) siRNA using a modified PEI as a gene carrier that specifically inhibit tumor growth and suppress tumor cell metastasis or the use of linear PEI for the intravenous delivery of transgene both *in vivo* and *in vitro* [22,23].

Herein, we hypothesized that co-delivery of small hairpin RNA (shRNA) against the anti-apoptotic gene, Bcl-xL, and the anti-cancer drug, DOX, in a single nanoplatform could provide superior therapeutic efficacy. Therefore, we synthesized aptamer-conjugated polyplexes (APs) that efficiently targeted delivery of shRNA and DOX to prostate cancer cells. In brief, branched polyethyleneimine was grafted to polyethylene glycol (PEI–PEG) as a shRNA delivery vehicle for Bcl-xL suppression. To this we conjugated an anti-PSMA aptamer (APT) that specifically bound prostate-specific membrane antigen (PSMA), which is presented on the cell surfaces of certain prostate cancer cells. Subsequently, DOX was intercalated into the APT and Bcl-xL-specific shRNA was complexed with the DOX intercalated PEI–PEG–APT conjugates (PEI–PEG–APT/DOX) to generate the APs (shRNA/PEI–PEG–APT/DOX). Fig. 1 shows the conceptual scheme for AP preparation and the synergistic effects of APs on cancer cells. We extensively evaluated the potential of APs to specifically and effectively drive prostate cancer cell death using fluorescence-activated cell sorting (FACS) analysis and cell viability tests.

2. Materials and methods

2.1. Materials

Branched polyethyleneimine (PEI, M_w: 25,000 Da) and N-(3-dimethylaminopropyl)-N′-ethylcarbodiimide hydrochloride (EDC) were purchased from Sigma–Aldrich. Sulfosuccinimidyl 4-(N-maleimidomethyl) cyclohexane-1-carboxylate (sulfo-SMCC) and N-hydroxysulfosuccinimide (sulfo-NHS) were purchased from Pierce. Doxorubicin hydrochloride and hetero bifunctional derivative of polyethylene glycol (SH-PEG-COOH, M_w: 3400 Da) were obtained from Fluka and Laysan Bio Inc., respectively. Lipofectamine™ 2000 was purchased from Invitrogen. The anti-PSMA aptamer (sequence: 5′-NH_2-spacer-GGGAGGACGAUGCGGAUCAGCCAUGUUUACGUCACUCCUUGUC-AAUCCUCAUCGGC invertedT-3′ with 2′-fluoro pyrimidines, 3′-inverted T cap, and 5′-amino group attached by a hexaethyleneglycol spacer) and nuclease-free water were obtained from Integrated DNA Technologies Inc. pEGFP-C1 (4.7 kb) was purchased from Clonetech Laboratories Inc. and purified using a Qiagen maxi-prep kit (QIAGEN, Germany). The Bcl-xL shRNA (sequence: CTCACTCTTCAGTCGGAAATGACCAGACA) and scrambled shRNA as a control (sequence: GCACTACCAGAGCTAACTCAGATAGTACT) were purchased from OriGene Technologies Inc. All other chemicals and reagents were of analytical grade.

2.2. Synthesis of PEI–PEG and PSMA aptamer-conjugated PEI–PEG (PEI–PEG–APT)

PEI–PEG was synthesized by conjugating branched polyethyleneimine (PEI) and hetero bifunctional polyethylene glycol (SH-PEG-COOH). PEI (0.8 μmol) was dissolved in 10 mL of ultrapure deionized (DI) water and was pre-activated with sulfo-SMCC (16 μmol) for 30 min. Subsequently, SH-PEG-COOH (8 μmol) was added to the solution and the reaction was carried out for 30 min. The product was filtered through an Amicon Ultra-15 (NMWL, nominal molecular weight limit: 5000) at 5000 g for 30 min to remove unreacted PEG and excess sulfo-SMCC. The purified PEI–PEG was lyophilized and stored at 4 °C for later use. The chemical structure of PEI–PEG was confirmed by Fourier-transform infrared spectroscopy (FT-IR, Varian, Excalibur™, USA) and an ^{1}H NMR spectrometer (JUM-ECP300, JEOL Ltd., Japan) with deuterium oxide as the solvent.

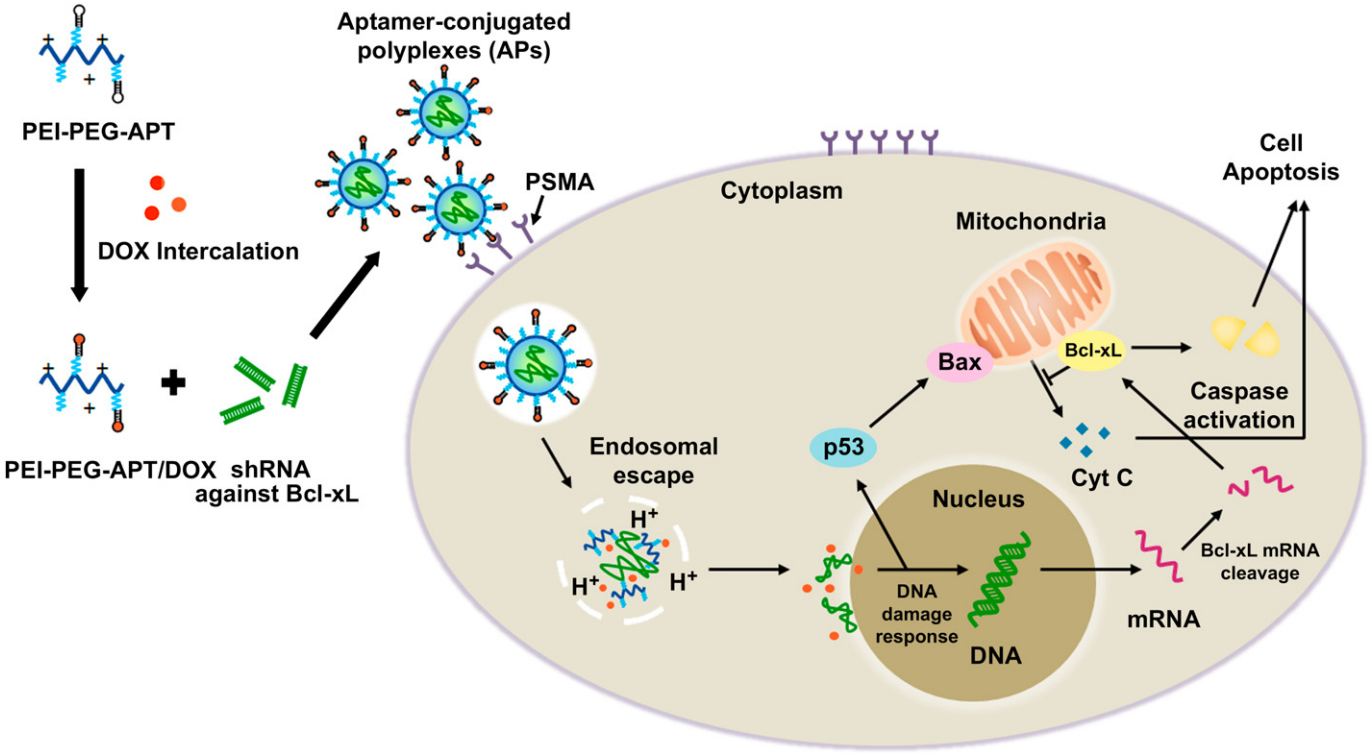

Fig. 1. Schematic illustration of co-delivery of shRNA and DOX using aptamer-conjugated polyplexes (APs).

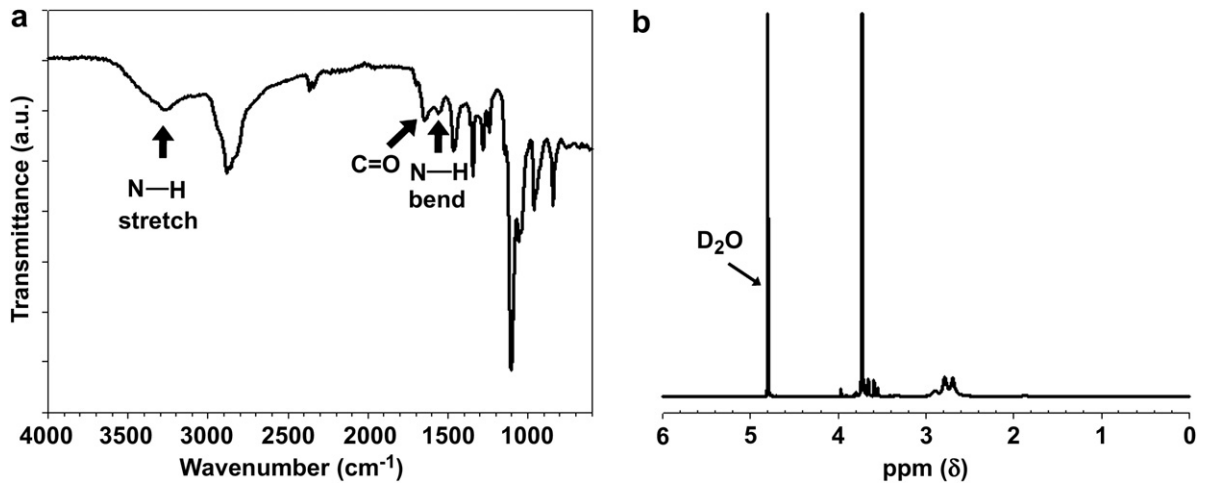

Fig. 2. (a) FT-IR and (b) ^{1}H NMR spectra of PEI–PEG conjugates.

To conjugate the anti-PSMA aptamer (APT) with PEI–PEG, 0.2 μmol PEI–PEG was dissolved in 3 mL nuclease-free water and was gently mixed with 0.2 μmol EDC and 0.2 μmol sulfo-NHS for 15 min at room temperature. The NHS-activated PEI–PEG was reacted with 0.02 μmol 5′-NH_2-modified APT for 4 h at 4 °C, and the resulting product was suspended in nuclease-free water without any further purification processes. The anti-PSMA aptamer-conjugated PEI–PEG (PEI–PEG–APT) was stored at 4 °C.

2.3. Preparation of doxorubicin (DOX)-loaded PEI–PEG–APT (PEI–PEG–APT/DOX)

The intercalation of DOX into APT was performed as reported [24]. A fixed concentration of DOX (2.5 μM) in nuclease-free water was added to a PEI–PEG–APT solution (molar ratio of DOX to APT 1:1 or 1:1.5) and to an APT solution (molar ratio of DOX to APT 1:1), which would act as a control, was gently shaken, and was then incubated at 4 °C for 30 min.

To confirm the quantity of intercalated DOX in the APT, the fluorescence spectra of the PEI–PEG–APT/DOX and APT/DOX were obtained at 500–750 nm (λ_{ex} = 480 nm, slit filter 10 nm, open) using a fluorescence spectrometer (LS55, Perkin Elmer, USA). The fluorescence intensities were measured at pre-determined time intervals of 2 h with varying pH (5.0, 7.4 and 9.0). For adjustment of pH, 0.1 N HCl and 0.1 N NaOH solutions were used.

2.4. Preparation of pEGFP/polymer complexes

pEGFP/polymer (pEGFP/PEI–PEG and pEGFP/PEI–PEG–APT) complexes were prepared by gentle mixing 3.5 μg of pEGFP in 250 μL of DI water with various amounts of polymer stock solution (1 mg/mL), corresponding to N/P ratios ranging from 1 to 25, into a final volume of 500 μL. The complexes were incubated for 20 min at room temperature prior to analysis.

Sizes and zeta potentials of the pEGFP/PEI–PEG–APT complexes formed in phosphate buffered saline (PBS, 10 mM, pH 7.4) at various N/P ratios (1–25) were measured in triplicate using laser scattering (ELS-Z, Otsuka electronics, Japan).

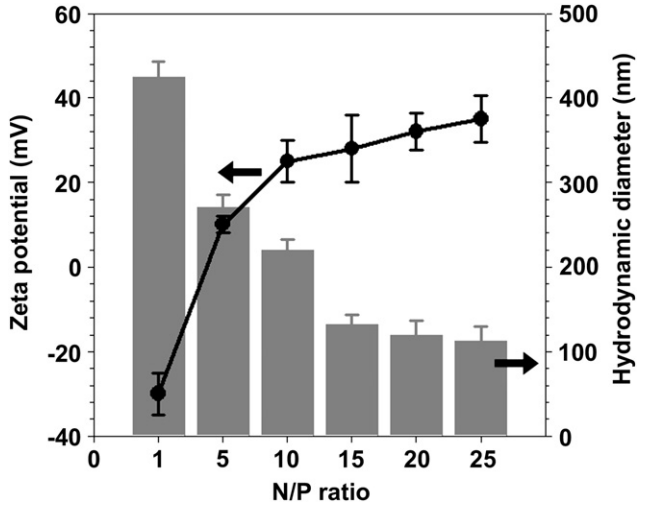

Fig. 3. Sizes and zeta potentials of pEGFP/PEI–PEG–APT complexes at various N/P ratios.

2.5. GFP expression analysis

The prostate carcinoma PC3 and LNCaP cell lines were obtained from American Tissue Type Culture (ATCC, USA) and were cultured in RPMI 1640 medium (Gibco, Invitrogen, USA) supplemented with 10% fetal bovine serum (FBS) and 1% antibiotics at 37 °C in a humidified atmosphere with 5% CO_2. Cells were seeded into six-well plates (Nunc., Thermo Fisher Scientific, USA) at a density of 3×10^5 (PC3) or 5×10^5 (LNCaP) cells per well and incubated at 37 °C for 24 h (to reach 70% confluence at the time of transfection) prior to transfection. The medium was replaced with 500 μL of serum-free medium and 500 μL of pEGFP/PEI–PEG–APT, and pEGFP/PEI–PEG complexes of different N/P ratios were added to each well. After 4 h of incubation, the medium was replaced with 2 mL of fresh medium containing serum and was incubated at 37 °C for an additional 48 h.

To evaluate the GFP expressions of the PEI–PEG and PEI–PEG–APT complexes according to N/P ratios in the PC3 and LNCaP cells, transfected cells were visualized with an epifluorescent microscope (IX 70, Olympus, Japan), and GFP expression was quantified by fluorescence-activated cell sorting (FACS) analysis (Becton Dickinson, Mountain View, USA). For FACS, the transfected cells were washed once with PBS (10 mM, pH 7.4) and detached by trypsinization. The collected cells were washed with FACS buffer (2% FBS and 0.02% NaN_3 in PBS), were resuspended in 200 μL of 4% paraformaldehyde, and were stored at 4 °C prior to FACS analysis. The relative transfection efficiency was quantified by dividing the number of GFP-expressing cells by the number of non-treated control cells. FACS analysis was repeated three times.

2.6. Western blot analysis

To assess the down-regulation of Bcl-xL gene in LNCaP cells, the cells were transfected with Bcl-xL shRNA/PEI–PEG–APT and scrambled shRNA/PEI–PEG–APT complexes, respectively. The cells were harvested at 24, 48 and 72 h post-transfection and lysed in cold RIPA buffer (50 mM Tris, pH 8.0, 150 mM NaCl, 1 mM EGTA, and 0.25% sodium deoxycholate). The lysates were incubated for 15 min at 4 °C and removed by centrifugation at 12,000 rpm for 15 min. Supernatants were analyzed for protein concentrations using the Bradford assay (Bio-Rad, Hercules, USA). Equal amount (10 μg) of protein was subjected to electrophoresis on sodium dodecyl sulphate (SDS)-polyacrylamide gels and then transferred to polyvinylidene fluoride (PVDF) membrane (Millipore, Billerica, USA). The blotted membranes were immunostained with antibodies specific for Bcl-xL antigens (Santa Cruz, Santa Cruz, USA). The signals were developed by a standard enhanced chemiluminescence (ECL) method according to the manufacture's protocol (Roche, Indianapolis, USA).

2.7. Time-dependent cell viability

To investigate the therapeutic efficacy of APs, we compared various Bcl-xL shRNA/polymer complexes (shRNA/Lipofectamine + DOX, pEGFP/PEI–PEG–APT/DOX, shRNA/PEI–PEG–APT, and shRNA/PEI–PEG–APT/DOX) that were prepared as previously described. We also used Lipofectamine™ 2000 as a control.

We evaluated the synergistic efficacy of combining anti-apoptotic gene silencing with the anti-cancer drug, AP (shRNA/PEI–PEG–APT/DOX), by measuring the

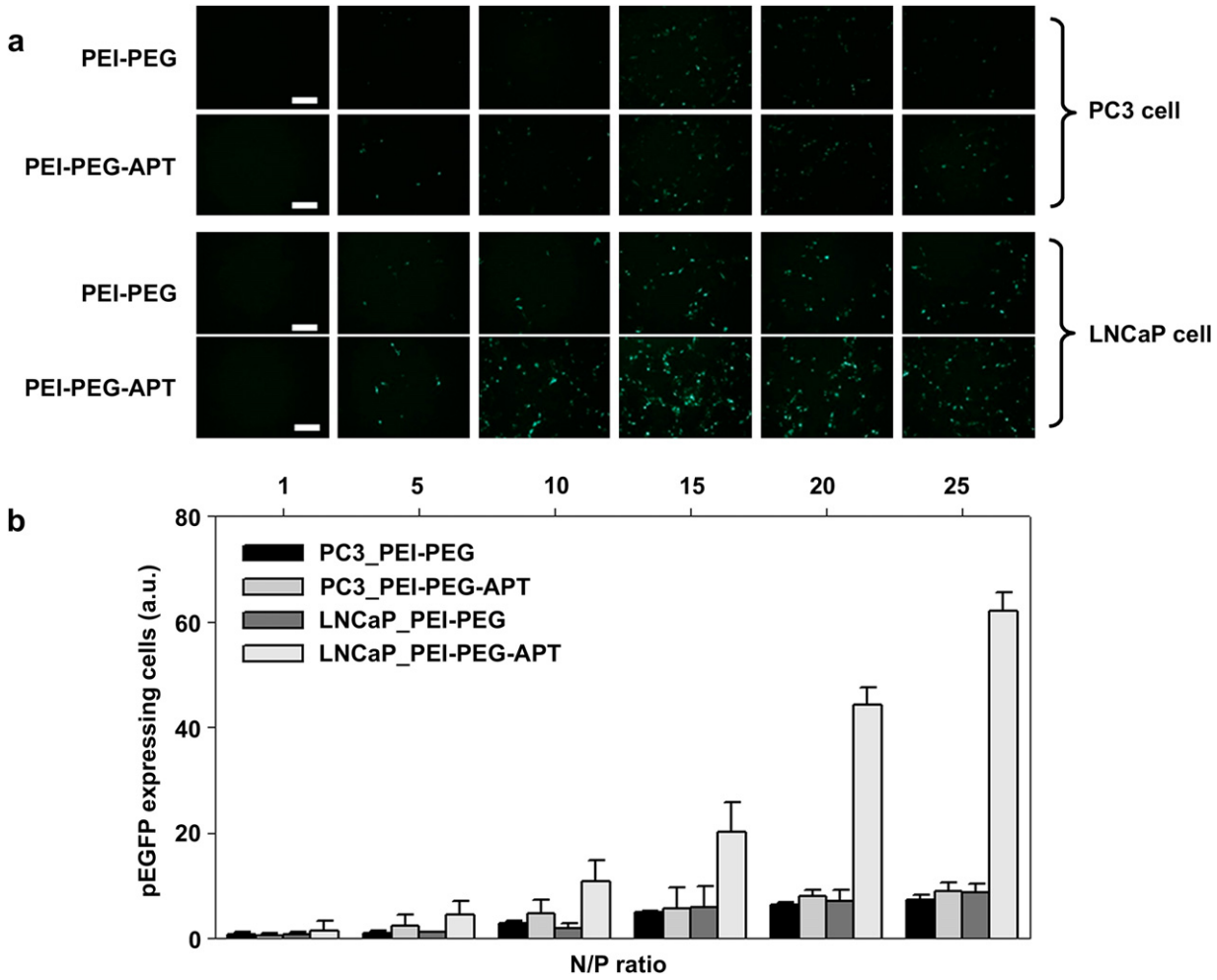

Fig. 4. (a) Fluorescence microscopy images (scale bar: 250 μm) and (b) FACS analysis ($n = 3$, error bars represent a standard deviation) after transfection of pEGFP/PEI–PEG or pEGFP/PEI–PEG–APT as a function of N/P ratios against PC3 and LNCaP cells, respectively.

inhibition of cell growth using the MTT [3-(4,5-dimethylthiazol-2-yl)-2,5-diphenyltetrazolium bromide] assay (Roche, Germany). Briefly, LNCaP cells were seeded in 96-microwell plates (Nunc, Thermo Fisher Scientific, USA) at a density of 1×10^4 cells per well and were incubated at 37 °C. After 24 h of incubation, the cells were treated with fresh medium (100 μL) containing shRNA/Lipofectamine + DOX, pEGFP/PEI–PEG–APT/DOX, shRNA/PEI–PEG–APT, or shRNA/PEI–PEG–APT/DOX. Cells were then incubated at 37 °C for 1, 2, 6, 12, 24, 36, 48, or 72 h. All experiments were performed in triplicate. Cell viability was determined from the ratio of treated cells to non-treated control cells.

2.8. In vitro anti-proliferation effect

The anti-proliferation effect of APs on PSMA-overexpressing prostate cancer cells, LNCaP cells, was evaluated using the MTT assay. LNCaP cells were plated in 96-microwell plates at a density of 1×10^4 cells per well and were incubated at 37 °C for 24 h. The cells were treated with various concentrations (0.03–32 μM) of pEGFP/PEI–PEG–APT/DOX, DOX, shRNA/Lipofectamine + DOX, or shRNA/PEI–PEG–APT/DOX and were then incubated at 37 °C for 48 h. Cell viability was measured as described previously. Each sample was tested in triplicate. The anti-proliferation effects were expressed as IC_{50} values, which represent the concentration that inhibits cell growth by 50% as compared with non-treated controls. IC_{50} values were calculated as $y = \text{Bottom} \times (\text{Top-Bottom})/[1 + 10^{(\log IC50 - x) \times \text{Hill slope}}]$, where Bottom and Top are the minimum and maximum y-axis values, respectively, of a plateau in the curve, and Hill slope is the steepness of the curve using GraphPad PRISM® (GraphPad Software Inc., USA).

3. Results and discussion

For the preparation of efficient intracellular delivery vehicles, branched PEI (polyethyleneimine) was grafted to PEG (polyethylene

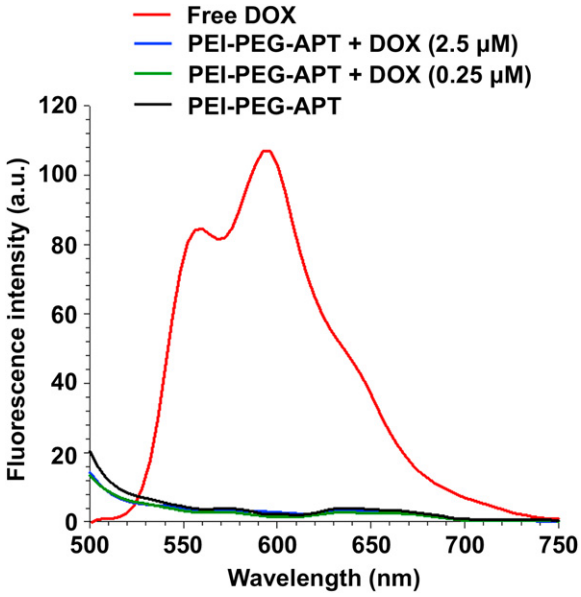

Fig. 5. Fluorescence intensity spectra of free DOX (2.5 μM), PEI–PEG–APT/DOX (molar ratio of APT to DOX 1:1 or 0.1:1), and PEI–PEG–APT ($\lambda_{ex} = 480$ nm).

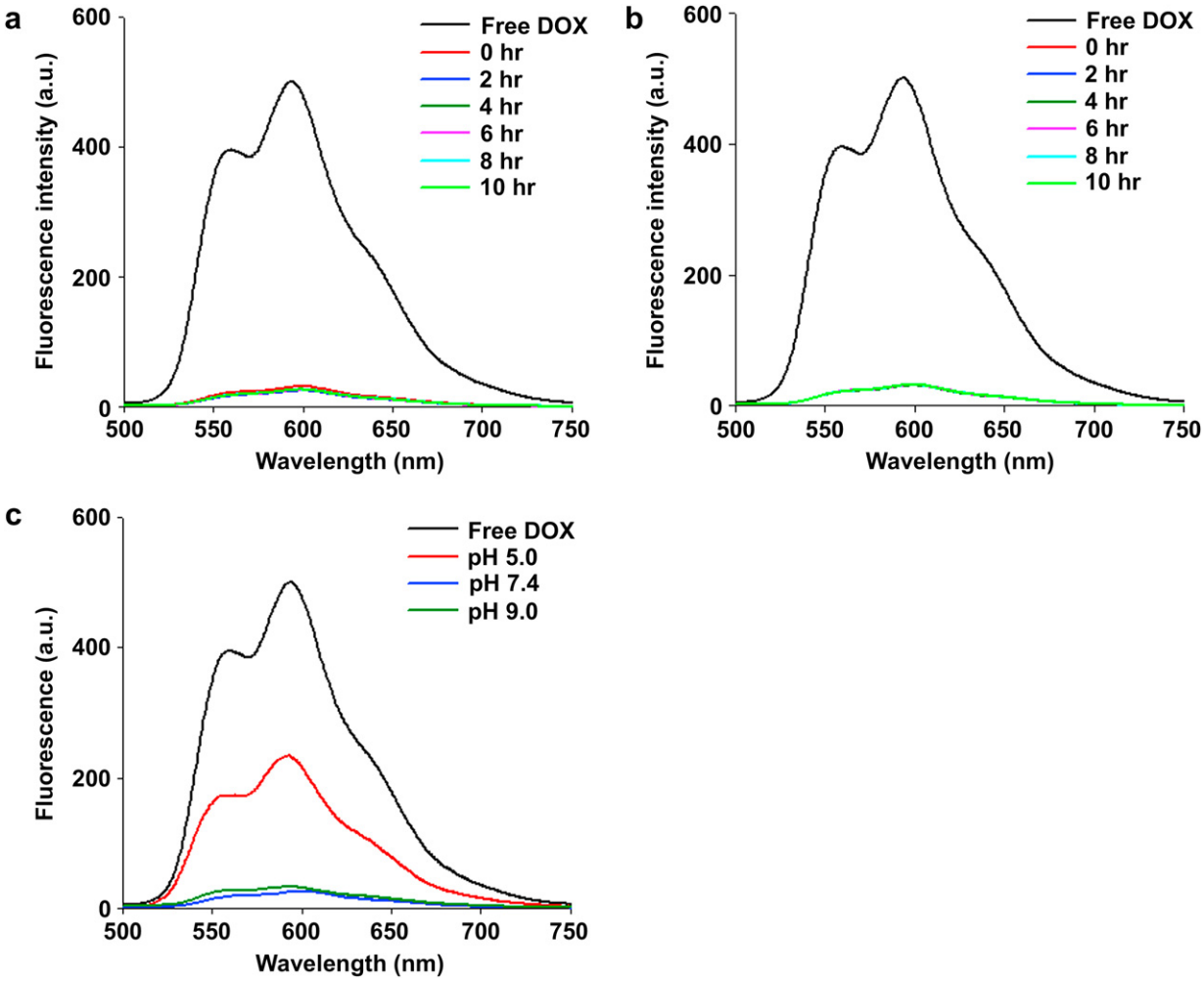

Fig. 6. Fluorescence intensity spectra of free DOX (2.5 μM) and APT/DOX after incubation of APT with DOX (λ_{ex} = 480 nm). Molar ratio of APT to DOX with a fixed concentration of DOX (2.5 μM); (a) 1.0 and (b) 1.5 at 2 h of time interval, and (c) pH-dependent fluorescence intensity spectra of APT/DOX at molar ratio of 1.0.

glycol) using a hetero bifunctional crosslinker (sulfo-SMCC). The primary amine groups of PEI were pre-activated with excess sulfo-SMCC and were covalently conjugated to the thiol group of the hetero bifunctional PEG derivatives (SH-PEG-COOH). After conjugation, the primary amine of PEI was coupled to the NHS ester of sulfo-SMCC to generate the amide bond between the PEI and PEG molecules. The characteristic peaks of the PEI–PEG conjugates from N-H-stretching bands (3500–3000 cm^{-1}), C=O–stretching bands (1660 cm^{-1}), and N–H–bending bands (1540 cm^{-1}) were confirmed by FT-IR spectroscopy (Fig. 2a). The chemical structure of the PEI–PEG conjugates was also evaluated from ^1H NMR spectroscopy, and the characteristic peaks were found at 3.65 ppm (–CH_2CH_2O– of PEG) and 2.8–2.6 ppm (–NH– and –NH_2 of PEI) (Fig. 2b). The degree of PEG grafting on branched PEI was 14.6, as determined by calculating the ratio of the number of protons in the –CH_2CH_2– peak of PEG to those in the –NH– or –NH_2– peaks of PEI. These results demonstrate that PEI–PEG was successfully synthesized as a gene delivery vehicle.

To selectively deliver gene and drug to prostate cancer cells, anti-PSMA aptamers (APTs) were conjugated with pre-synthesized PEI–PEG using EDC/NHS chemistry. Briefly, the carboxyl group of PEI–PEG was pre-activated with N-(3-dimethylaminopropyl)-N′-ethylcarbodiimide hydrochloride (EDC) and N-hydroxysulfosuccinimide (sulfo-NHS) with the same molar ratio of EDC/sulfo-NHS to form an NHS ester and was then reacted with 5′-NH_2-modified APT at a molar ratio of 0.1 to PEI–PEG. Thus, we assumed that the added APT was completely conjugated to PEI–PEG because the amount of treated activation agents was 10-fold larger than the APT molecules.

Plasmid DNA was condensed with PEI–PEG–APT via electrostatic interactions between polycationic PEI and polyanionic plasmid DNA. The characteristics of the complexes (i.e., size, transfection efficiency, and cytotoxicity) were influenced by condensability, therefore, a proper N/P ratio (the number of PEI nitrogen residues per the number of plasmid DNA phosphate groups) should be determined to form the most stable and compact vehicles for efficient gene delivery [25–28]. The sizes and zeta

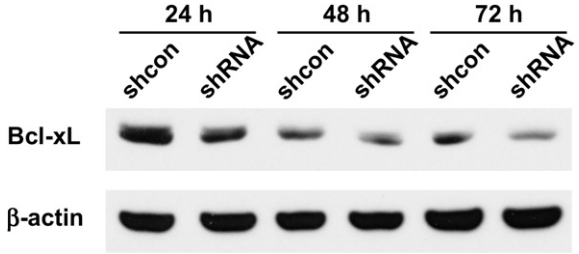

Fig. 7. Bcl-xL knocks down following shRNA/PEI–PEG–APT complexes delivery to LNCaP cells. The cells were treated with Bcl-xL shRNA/PEI–PEG–APT (shRNA) and scrambled shRNA/PEI–PEG–APT (shcon) complexes and processed for immunoblotting with anti-Bcl-xL antibodies at 24, 48, and 72 h post-transfection. β-actin was a loading control.

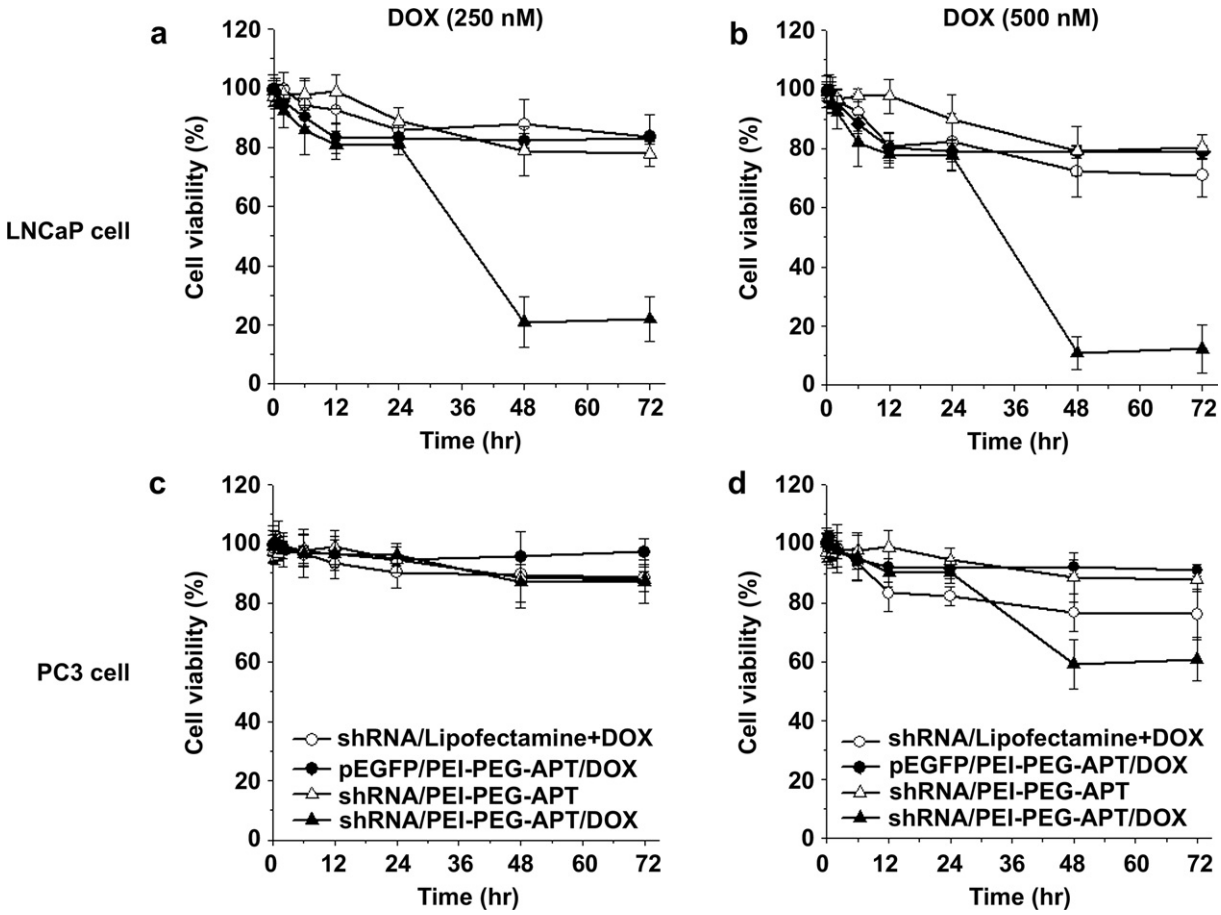

Fig. 8. Time-dependent cell viabilities of (a, b) LNCaP cells and (c, d) PC3 cells against shRNA/Lipofectamine + DOX, pEGFP/PEI–PEG–APT/DOX, shRNA/PEI–PEG–APT, and shRNA/PEI–PEG–APT/DOX ($n = 3$, error bars represent a standard deviation).

potentials of the pEGFP/PEI–PEG–APT complexes were analyzed using laser scattering over a range of N/P ratios (Fig. 3). As shown in Fig. 3, the sizes of the pEGFP/PEI–PEG–APT complexes decreased and the zeta potentials increased as the N/P ratios increased. At high N/P ratios, the small size resulted from the formation of more compact structures owing to the higher ionic interactions and the net electrostatic repulsive forces between complexes. The strong positive charges of the complexes provided higher transfection efficiency but can also induced cytotoxicity by disrupting and solubilizing cell membranes [29], thus, PEG was conjugated to PEI as a non-cytotoxic gene carrier.

To investigate targeted delivery and transfection efficiency of PEI–PEG–APT in PSMA-overexpressing cells, LNCaP cells and PC3 cells were treated with pEGFP/PEI–PEG and pEGFP/PEI–PEG–APT complexes in a range of N/P ratios using 3.5 μg of pEGFP. GFP expression was analyzed using fluorescence microscopy (Fig. 4a). In LNCaP cells, pEGFP/PEI–PEG–APT complexes resulted in higher GFP fluorescence than in the pEGFP/PEI–PEG complexes, whereas GFP fluorescence was rarely observed in PC3 cells transfected by pEGFP/PEI–PEG–APT complexes. To determine the optimal N/P ratio, GFP fluorescence intensity was examined at varying N/P ratios. In Fig. 4a, GFP intensities of the PEI–PEG–APT complexes transfected with LNCaP cells increased with N/P ratio, while PC3 cells exhibited insignificant differences. Furthermore, GFP expression was quantified by comparing the number of GFP-expressing cells in the test and control cells using FACS analysis. As shown in Fig. 4b, the transfection efficiency of PEI–PEG–APT was three-fold higher than that of PEI–PEG in LNCaP cells at an N/P ratio of 15, but no difference was observed in PC3 cells. These results suggest that the pEGFP/PEI–PEG–APT complexes could enhance the transfection efficiency in the LNCaP cells via APT-specific targeting. The cytotoxicity of both complexes was observed over an N/P ratio of 20 in both the PC3 and LNCaP cells (data not shown). Consequently, we set the optimal N/P ratio at 15 for the synthesis of pEGFP/PEI–PEG–APT complexes to balance high GFP expression with the absence of cytotoxicity.

To assess the intercalation of DOX into APT, the fluorescence intensities of the free DOX, PEI–PEG–APT/DOX, and PEI–PEG solutions were measured using a fluorescence spectrometer. Π-electrons of DOX have been known to interact with two base pairs of DNA by intercalation without chemical conjugation due to its planar aromatic ring structure [30]. Thus, DOX can intercalate with APT containing short oligonucleotides [31–33]. DOX which has intercalated into APT may release from APT by simple diffusion or through APT degradation by endonucleases in the lysosomes [24,34]. Spectrometrically, DOX is excited at 480 nm and fluoresces at 500–750 nm. When DOX molecules were intercalated into APT, however, its fluorescence was quenched. As shown in Fig. 5, free DOX (2.5 μM) exhibited the maximum emission at 590 nm, while PEI–PEG–APT/DOX (molar ratio of APT to DOX 1:1 or 1:0.1) resulted in fluorescence quenching. Therefore, we measured the changes in fluorescence intensity of the APT/DOX solutions at regular time intervals after intercalation of DOX with APT (APT/DOX). In Fig. 6a and b, the fluorescence intensity of APT/DOX (molar ratio of APT to DOX 1:1 or 1:1.5) compared to that of the free DOX (2.5 μM) rapidly decreased and then changed little with time, indicating that DOX was not simply released by diffusion. Therefore we expected a relatively sustainable release because DOX/APT was

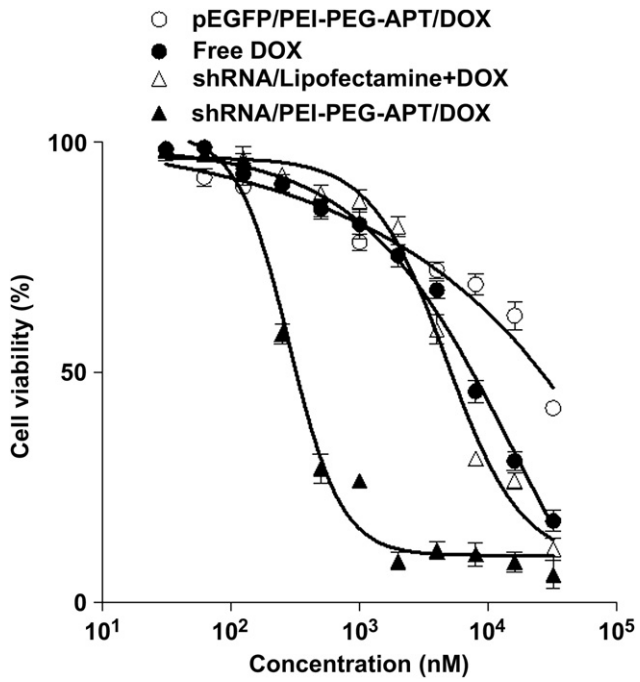

Fig. 9. Cell viabilities of LNCaP cells treated with pEGFP/PEI–PEG–APT/DOX, free DOX, shRNA/Lipofectamine + DOX, and shRNA/PEI–PEG–APT/DOX (n = 3, error bars represent a standard deviation).

stably complexed. Subsequently, we adjusted the pH of ATP/DOX solutions (pH 5.0, 7.4, and 9.0) and analyzed the fluorescence of these APT/DOX solutions. While the fluorescence intensity of DOX increased up to 50% of that of the free DOX in an acidic environment (pH 5.0), the fluorescence was quenched in neutral (pH 7.4) or basic environments (pH 9.0), verifying that DOX could be released due to APT deactivation under acidic conditions because of its solubility increases by the protonation of a primary amine group of DOX at low pH. Hence, we anticipated that after internalization of APs into cancer cells, DOX would be released via APT deactivation resulting from endosomal acidic pH and shRNA would simultaneously escape from the endosome due to the proton sponge effect and then translocate to the nucleus.

To investigate whether PEI–PEG–APT mediated delivery of shRNA results in knock down of target gene, Bcl-xL, the protein levels were assessed at 24, 48, and 72 h following the transfection. LNCaP cells were treated with Bcl-xL shRNA/PEI–PEG–APT and scrambled shRNA/PEI–PEG–APT complexes as a control, respectively. The expression of Bcl-xL protein began to decrease after 48 h of shRNA transfection and was significantly decreased after 72 h (Fig. 7). Thus, down-regulation of Bcl-xL gene by the delivery of shRNA is expected to increase cell apoptosis due to its key role in the regulation of apoptosis that enhances cell survival by suppressing apoptosis in a variety of cells subject to death signals [35–37].

To form aptamer-conjugated polyplexes (APs) for selectively targeting DOX and shRNA to specific cancer cells, the intercalated DOX with anti-PSMA aptamer-conjugated polycationic polymer (PEI–PEG–APT/DOX) was finally complexed with shRNA against the anti-apoptotic Bcl-xL gene. When DNA is damaged by DOX, p53 protein levels will stabilize, resulting in an up-regulation of Bax. Bax induces the release of cytochrome c into the cytosol, followed by activation of the intrinsic apoptotic pathway [38,39]. Accordingly, we expected synergistic cell death from both DOX-mediated Bax up-regulation and shRNA-mediated Bcl-xL down-regulation. Therefore, we evaluated the cytotoxic effects of APs on LNCaP and PC3 cells using the MTT assay. At very low concentrations of DOX (250 nM) which resulted in 85% cell viability in both cell types (data not shown), APs (shRNA/PEI–PEG–APT/DOX) remarkably increased cytotoxicity in LNCaP cells compared to the treatments using only shRNA-loaded polyplexes (shRNA/PEI–PEG–APT), only DOX-loaded polyplexes (pEGFP/PEI–PEG–APT/DOX), or shRNA complexed with Lipofectamine™ 2000 plus free DOX (shRNA/Lipofectamine + DOX) (Fig. 8a and b). In contrast, PC3 cells treated with APs underwent no cytotoxicity (Fig. 8c and d). In Fig. 8a, the cell viability of LNCaP cells rapidly decreased from 81% to 21% after 48 h of AP treatment. Of note, nanoparticles containing only DOX were more cytotoxic to LNCaP cells at 12 h of incubation than were those only containing shRNA, suggesting that DOX released from APTs can induce minor cell death by inducing the DNA damage-response. After 48 h of AP treatment, shRNA may begin to down-regulate Bcl-xL, and thus, synergizing with DOX to activate the intrinsic apoptotic pathway. Treatment with 500 nM DOX was more cytotoxic in LNCaP and PC3 cells also treated with APs than treatment with 250 nM DOX due to the non-specific cytotoxicity of the increased DOX concentration (Fig. 8b and d).

To assess the anti-proliferative effect of APs, the dose-dependent effects on LNCaP cell viability was measured using the MTT assay, and IC_{50} values were determined. Treatment of LNCaP cells with pEGFP/PEI–PEG–APT/DOX, free DOX, shRNA/Lipofectamine + DOX, or shRNA/PEI–PEG–APT/DOX (APs) (0.03–32 μM) inhibited cell growth in a dose-dependent manner (Fig. 9). The calculated IC_{50} values were 102.0, 16.8, 4.7 and 0.3 μM, respectively. Thus, APs had an approximately 17-fold lower IC_{50} value than that of the simple mixture of drug and gene (shRNA/Lipofectamine + DOX), indicating that APs loaded with both DOX and shRNA significantly increase cytotoxicity compared to treatment where the therapeutics are simply mixed.

4. Conclusions

We successfully fabricated aptamer-conjugated polyplexes (APs) to synergistically induce selective cell death of prostate cancer cells. The APs consisted of Bcl-xL-specific shRNA complexed with PEI–PEG–APT conjugates and DOX loaded into an APT in order to activate intrinsic apoptosis. Our nanoplatform efficiently and selectively delivered both shRNA and anti-cancer drug to LNCaP cells through aptamer-mediated binding to PSMA which is expressed on the cell surfaces. Moreover, the shRNA- and DOX-laden APs had excellent tumoricidal efficacy as verified by cell viability assays. This study greatly contributes to the use of nanocarrier-based delivery of different therapeutic modalities for the synergistic treatment of cancer.

Acknowledgments

This study was supported by a grant of the Korea Health 21 R&D Project, Ministry of Health &Welfare, Republic of Korea (A085136). This work was supported by the Korea Science and Engineering Foundation (KOSEF) grant funded by the Korea government (MOST) (No. 2007-04045). This study was supported by a faculty research grant of Yonsei University College of Medicine (6-2007-0198).

Appendix

Figures with essential colour discrimination. Figs. 1, 4, 5, 6 in this article have parts that may be difficult to interpret in black and white. The full colour images can be found in the on-line version, at doi:10.1016/j.biomaterials.2010.02.030.

References

[1] Frei E. Combination cancer therapy: presidential address. Cancer Res 1972;32:2593–607.

[2] Walsh C. Molecular mechanisms that confer antibacterial drug resistance. Nature 2000;406:775–81.
[3] Hanahan D, Bergers G, Bergsland E. Less is more, regularly: metronomic dosing of cytotoxic drugs can target tumor angiogenesis in mice. J Clin Invest 2000;105:1045–7.
[4] Hongrapipat J, Kopeckova P, Liu J, Prakongpan S, Kopecek J. Combination chemotherapy and photodynamic therapy with Fab' fragment targeted HPMA copolymer conjugates in human ovarian carcinoma cells. Mol Pharm 2008;5:696–709.
[5] Wiradharma N, Tong YW, Yang Y. Self-assembled oligopeptide nanostructures for co-delivery of drug and gene with synergistic therapeutic effect. Biomaterials 2009;30:3100–9.
[6] Lee H, Hu M, Reilly RM, Allen C. Apoptotic epidermal growth factor (EGF)-conjugated block copolymer micelles as a nanotechnology platform for targeted combination therapy. Mol Pharm 2007;4:769–81.
[7] Griscelli F, Li H, Cheong C, Opolon P, Bennaceur-Griscelli A, Vassal G, et al. Combined effects of radiotherapy and angiostatin gene therapy in glioma tumor model. Proc Natl Acad Sci USA 2000;97:6698–703.
[8] Pederson LC, Buchsbaum DJ, Vickers SM, Kancharla SR, Mayo MS, Curiel DT, et al. Molecular chemotherapy combined with radiation therapy enhances killing of cholangiocarcinoma cells in vitro and in vivo. Cancer Res 1997;57:4325–32.
[9] Raben D, Helfrich B, Chan DC, Ciardiello F, Zhao L, Franklin W, et al. The effects of cetuximab alone and in combination with radiation and/or chemotherapy in lung cancer. Clin Cancer Res 2005;11:795–805.
[10] Pegram M, Hsu S, Lewis G, Pietras R, Beryt M, Sliwkowski M, et al. Inhibitory effects of combinations of HER-2/neu antibody and chemotherapeutic agents used for treatment of human breast cancers. Oncogene 1999;18:2241–51.
[11] Chow KU, Sommerlad WD, Boehrer S, Schneider B, Seipelt G, Rummel MJ, et al. Anti-CD20 antibody (IDEC-C2B8, rituximab) enhances efficacy of cytotoxic drugs on neoplastic lymphocytes in vitro: role of cytokines, complement, and cAPases. Haematologica 2002;87:33–43.
[12] Yang J, Lee CH, Ko HJ, Suh JS, Yoon HG, Lee K, et al. Multifunctional magneto-polymeric nanohybrids for targeted detection and synergistic therapeutic effects on breast cancer. Angew Chem-Int Edit 2007;119:8992–5.
[13] Cho K, Wang X, Nie S, Chen Z, Shin DM. Therapeutic nanoparticles for drug delivery in cancer. Clin Cancer Res 2008;14:1310–6.
[14] Janat-Amsbury MM, Yockman JW, Lee M, Kern S, Furgeson DY, Bikram M, et al. Combination of local, nonviral IL12 gene therapy and systemic paclitaxel treatment in a metastatic breast cancer model. Mol Ther 2004;9:829–36.
[15] MacDiarmid JA, Amaro-Mugridge NB, Madrid-Weiss J, Sedliarou I, Wetzel S, Kochar K, et al. Sequential treatment of drug-resistant tumors with targeted minicells containing siRNA or a cytotoxic drug. Nat Biotechnol 2009;27:643–51.
[16] Dong X, Liu A, Zer C, Feng J, Zhen Z, Yang M, et al. siRNA inhibition of telomerase enhances the anti-cancer effect of doxorubicin in breast cancer cells. BMC Cancer 2009;9:133–42.
[17] Wang Y, Gao S, Ye W, Yoon HS, Yang Y. Co-delivery of drugs and DNA from cationic core-shell nanoparticles self-assembled from a biodegradable copolymer. Nat Mater 2006;5:791–6.
[18] Beh CW, Seow WY, Wang Y, Zhang Y, Ong ZY, Ee PLR, et al. Efficient delivery of Bcl-2-targeted siRNA using cationic polymer nanoparticles: downregulating mRNA expression level and sensitizing cancer cells to anticancer drug. Biomacromolecules 2008;10:41–8.
[19] Lima RT, Martins LM, Guimaraes JE, Sambade C, Vasconcelos MH. Specific downregulation of bcl-2 and xIAP by RNAi enhances the effects of chemotherapeutic agents in MCF-7 human breast cancer cells. Cancer Gene Ther 2004;11:309–16.
[20] Nagamatsu K, Tsuchiya F, Oguma K, Maruyama H, Kano R, Hasegawa A. The effect of small interfering RNA (siRNA) against the Bcl-2 gene on apoptosis and chemosensitivity in a canine mammary gland tumor cell line. Res Vet Sci 2008;84:49–55.
[21] Urban-Klein B, Werth S, Abuharbeid S, Czubayko F, Aigner A. RNAi-mediated gene-targeting through systemic application of polyethylenimine (PEI)-complexed siRNA in vivo. Gene Ther 2004;12(5):461–6.
[22] Li S, Dong W, Zong Y, Yin W, Jin G, Hu Q, et al. Polyethylenimine-complexed plasmid particles targeting focal adhesion kinase function as melanoma tumor therapeutics. Mol Ther 2007;15(3):515–23.
[23] Goula D, Benoist C, Mantero S, Merlo G, Levi G, Demeneix BA. Polyethylenimine-based intravenous delivery of transgenes to mouse lung. Gene Ther 1998;5(9):1291–5.
[24] Bagalkot V, Zhang L, Levy-Nissenbaum E, Jon S, Kantoff PW, Langer R, et al. Quantum dot-aptamer conjugates for synchronous cancer imaging, therapy, and sensing of drug delivery based on bi-fluorescence resonance energy transfer. Nano Lett 2007;7:3065–70.
[25] Nguyen HK, Lemieux P, Vinogradov SV, Gebhart CL, Guerin N, Paradis G, et al. Evaluation of polyether–polyethyleneimine graft copolymers as gene transfer agents. Gene Ther 2000;7:126–38.
[26] Park MR, Han KO, Han IK, Cho M, Nah JW, Choi YJ, et al. Degradable polyethylenimine-alt-poly(ethylene glycol) copolymers as novel gene carriers. J Control Release 2005;105:367–80.
[27] Mao S, Neu M, Germershaus O, Merkel O, Sitterberg J, Bakowsky U, et al. Influence of polyethylene glycol chain length on the physicochemical and biological properties of poly(ethylene imine)-graft-poly(ethylene glycol) block copolymer/siRNA polyplexes. Bioconjugate Chem 2006;17:1209–18.
[28] Jiang H, Kim Y, Arote P, Nah J, Cho M, Choi Y, et al. Chitosan-graft-polyethylenimine as a gene carrier. J Control Release 2007;117:273–80.
[29] Fischer D, Li Y, Ahlemeyer B, Krieglstein J, Kissel T. In vitro cytotoxicity testing of polycations: influence of polymer structure on cell viability and hemolysis. Biomaterials 2003;24:1121–31.
[30] Liu Z, Sun X, Nakayama-Ratchford N, Dai H. Supramolecular chemistry on water-soluble carbon nanotubes for drug loading and delivery. ACS Nano 2007;1:50–6.
[31] Qu X, Wan C, Becker H, Zhong D, Zewail AH. The anticancer drug-DNA complex: femtosecond primary dynamics for anthracycline antibiotics function. Proc Natl Acad Sci USA 2001;98:14212–7.
[32] Wochner A, Menger M, Orgel D, Cech B, Rimmele M, Erdmann VA, et al. A DNA aptamer with high affinity and specificity for therapeutic anthracyclines. Anal Biochem 2008;373:34–42.
[33] Bagalkot V, Lee I, Yu MK, Lee E, Park S, Lee J, et al. A combined chemo-immunotherapy approach using a plasmid–doxorubicin complex. Mol Pharm 2009;6:1019–28.
[34] Bagalkot V, Farokhzad OC, Langer R, Jon S. An aptamer–doxorubicin physical conjugate as a novel targeted drug-delivery platform. Angew Chem-Int Edit 2006;118:8329–32.
[35] Cory S, Adams JM. The Bcl2 family: regulators of the cellular life-or-death switch. Nat Rev Cancer 2002;2(9):647–56.
[36] Jiang M, Milner J. Bcl-2 constitutively suppresses p53-dependent apoptosis in colorectal cancer cells. Genes Dev 2003;17(7):832–7.
[37] Wang R, Lin F, Wang X, Gao P, Dong K, Wei S, et al. Suppression of Bcl-xL expression by a novel tumor-specific RNA interference system inhibits proliferation and enhances radiosensitivity in prostatic carcinoma cells. Cancer Chemother Pharmacol 2008;61(6):943–52.
[38] Nithipongvanitch R, Ittarat W, Velez JM, Zhao R, Clair DKS, Oberley TD. Evidence for p53 as guardian of the cardiomyocyte mitochondrial genome following acute adriamycin treatment. J Histochem Cytochem 2007;55:629–39.
[39] Sardao VA, Oliveira PJ, Holy J, Oliveira CR, Wallace KB. Doxorubicin-induced mitochondrial dysfunction is secondary to nuclear p53 activation in H9c2 cardiomyoblasts. Cancer Chemother Pharmacol 2009;64:811–27.